

1 **Quantitative longitudinal predictions of Alzheimer's disease by multi-modal predictive**
2 **learning**

3
4 Prakash, M.^{1, *}, Abdelaziz, M.², Zhang, L.³, Strange, B.A.,^{3,4}, Tohka, J.¹, for the Alzheimer's
5 Disease Neuroimaging Initiative. ^{**}

6
7 mithilesh.prakash@uef.fi

8 mahmoudabdelaziz@gmail.com

9 zhangl87@connect.hku.hk

10 bryan.strange@upm.es

11 jussi.tohka@uef.fi

12

- 13 1. University of Eastern Finland, A.I. Virtanen Institute for Molecular Sciences, Kuopio, Finland
14 2. Zewail City of Science and Technology, Giza, Egypt
15 3. Department of Neuroimaging, Alzheimer's Disease Research Centre, Reina Sofia-CIEN
16 Foundation, Madrid, Spain
17 4. Laboratory for Clinical Neuroscience, CTB, Universidad Politécnica de Madrid, Madrid, Spain

18

19

20

21 ***Corresponding Author:**

22 Mithilesh Prakash, PhD

23 A.I. Virtanen Institute for Molecular Sciences

24 University of Eastern Finland

25 P.O.B. 1627

26 FI-70211 Kuopio, Finland

27 mithilesh.prakash@uef.fi

28

29 ^{**} Data used in the preparation of this article were obtained from the Alzheimer's Disease
30 Neuroimaging Initiative ([ADNI](#)) database.

31

32 **Abstract**

33 **Background:** Quantitatively predicting the progression of Alzheimer's disease (AD) in an
34 individual on a continuous scale, such as AD assessment scale-cognitive (ADAS-cog) scores, is
35 informative for a personalized approach as opposed to qualitatively classifying the individual into a
36 broad disease category. We hypothesize that multi-modal data and predictive learning models can
37 be employed for longitudinally predicting ADAS-cog scores.

38 **Methods:** Multivariate regression techniques were employed to model baseline multi-modal data
39 (demographics, neuroimaging, and cerebrospinal fluid based markers, and genetic factors) and
40 future ADAS-cog scores. Prediction models were subjected to repeated cross-validation and the
41 resulting mean absolute error and cross-validated correlation of the model assessed.

42 **Results:** Prediction models on multi-modal data outperformed single modal data up to 36 months.
43 Incorporating baseline ADAS-cog scores to prediction models marginally improved predictive
44 performance.

45 **Conclusions:** Future ADAS-cog scores were successfully estimated via predictive learning aiding
46 clinicians in identifying those at greater risk of decline and apply interventions at an earlier disease
47 stage and inform likely future disease progression in individuals enrolled in AD clinical trials.

48 **Keywords:** Alzheimer's disease, Magnetic resonance imaging, Machine Learning,
49 Neuropsychology, Multivariate, PLS, ADAS-cog

50

51 **1 Background**

52 Alzheimer's disease (AD) is an irreversible and multi-factorial neurodegenerative disease with a
53 progressive decline in cognitive abilities [1]. AD affects several tens of millions of people globally.
54 Yet, the pathogenesis of AD remains unclear [2]. Cognitive tests, brain volumetry from magnetic
55 resonance imaging (MRI), amyloid load and glucose consumption levels from positron emission
56 tomography (PET), and protein analysis of cerebrospinal fluid (CSF) provide valuable and
57 complementary disease markers to chart the disease progression [3]. Qualitative manual analysis of
58 these markers to diagnose patients could be potentially aided by automated algorithms.

59
60 The classification based on clinical diagnosis places an individual into normal, mild cognitive
61 impairment (MCI), or AD groups [4]. Memory loss (either self-reported or by an associate) is
62 observed during the initial stages of AD [5]. Declining cognitive skills is also common and can
63 potentially lead to dementia [6]. Hence, it is imperative that the disease progression is carefully
64 monitored at the earliest stages [7]. AD risk factors include sociodemographic factors (e.g.,
65 increasing age and fewer years of education), genetic (APOE expression) and patient medical and
66 family history [8]. A clinical diagnosis of AD is currently a challenge due to lack of clear diagnostic
67 markers of AD, and overlapping clinical features with other dementia types. However at post-
68 mortem, AD is characterized by the presence of amyloid β -peptide plaques and accumulations of τ
69 proteins in the brain histology samples [9].

70
71 The progressive nature of AD makes diagnosing an individual into any of the discrete groups a
72 challenging proposition [10,11]. Conventional progression tracking analyzes clinical changes in
73 MRI, CSF and cognitive biomarkers [12,13], but this could be inefficient as the changes can be
74 slow and difficult to detect [14,15]. The change in these biomarkers is nonlinear with AD's
75 progression, further complicating longitudinal tracking. Therefore, quantifying and tracking the

76 condition of the patient by continuous measures such as ADAS-cog scores has been advocated
77 [16,17]. ADAS-cog is widely used clinically (to measure language, memory, praxis, and other
78 cognitive abilities) and provides an accurate description of the cognitive state on a continuous scale,
79 making it an ideal choice in our study [18,19]. The availability of standardized multi-modal data
80 and corresponding longitudinal ADAS-cog scores from research organizations, such as the
81 Alzheimer's Disease Neuroimaging Initiative (ADNI) project, has enabled the development of
82 novel techniques for tracking AD progression by employing machine learning [20]. However,
83 predicting ADAS-cog scores has been reported as very difficult [21]. In the recent Alzheimer's
84 Disease Prediction of Longitudinal Evolution (TADPOLE) Challenge ([https://tadpole.grand-](https://tadpole.grand-challenge.org/)
85 [challenge.org/](https://tadpole.grand-challenge.org/)), forecasts of clinical diagnosis and ventricle volume were very good, whereas, for
86 ADAS-cog, no team participating in the challenge was able to generate forecasts that were
87 significantly better than chance.

88
89 Multivariate regression techniques, such as partial least squares regression (PLSR), support-vector
90 regression (SVR) and random forest regression, enable modeling complex relationships between
91 baseline multi-modal ADNI data (predictors) with future ADAS-cog 13 scores [22,23]. The
92 multivariate nature of the modeling is desirable for the ADAS-cog score trajectory analysis due to
93 the complementary nature of the AD measures. The resulting trajectory predictions could alert
94 clinicians to prescribe appropriately (once disease modifying interventions are available).
95 Moreover, knowing the likely future trajectory of the disease will provide a benchmark with which
96 to test clinical evolution in patients enrolled in clinical trials.

97
98 We hypothesized that the multivariate regression techniques are well suited for multi-factorial
99 diseases and that the progression of AD, as indicated by ADAS-cog scores in subsequent timelines,

100 can be accurately predicted. Furthermore, the inclusion of baseline ADAS-cog scores could
101 improve the predictions of the model in subsequent follow-ups.

102

103 **2 Methods**

104 **2.1 ADNI Dataset**

105 Data in this study were obtained from the Alzheimer’s Disease Neuroimaging Initiative (ADNI)
106 database (<http://adni.loni.usc.edu/>). In addition to the various summary tables directly provided by
107 ADNI, we used summary tables prepared for the TADPOLE grand challenge based on ADNI data
108 at <https://tadpole.grand-challenge>) [21,24]. The data are from the TADPOLE tables if not otherwise
109 stated. Specific variable names are provided as supplementary Table S.1. The ADNI project started
110 in 2003 as a public-private partnership, led by PI Michael W. Weiner, MD. The main objective of
111 ADNI is to evaluate the application of serial magnetic resonance imaging (MRI), positron emission
112 tomography (PET), other biological markers, and clinical and neuropsychological assessment in a
113 multi-modal approach to determine the longitudinal progression of mild cognitive impairment
114 (MCI) and early Alzheimer’s disease (AD). We utilized pre-processed ADNI data because of the
115 standardized processing pipeline that ensured the quality of the data. This multimodal data is readily
116 available for other researchers enabling a direct comparison of the study results. Readers are
117 directed to www.adni-info.org for detailed information on the ADNI project and the TADPOLE
118 challenge <https://tadpole.grand-challenge.org> constructed by the EuroPOND consortium
119 (<http://europond.eu>).

120

121 **2.1.1 Subjects**

122 The characteristics of subjects recruited in the ADNI dataset are described in detail here
123 <http://adni.loni.usc.edu/>. The trends of the ADAS-cog 13 scores utilized in this study are provided
124 in Figure S.1 and the details of subject characteristics are provided in Table S.2 of the

125 supplementary section. There are fewer subjects in follow-up visits than in the baseline visit due to
126 subject attrition and missing data. Note that some subjects change diagnostic status over the follow-
127 up period. The roster identification (RID) numbers of the included subjects are provided as comma-
128 separated values in the supplementary section.

129

130 **2.1.2 MRI**

131 As MRI features, we used 9 features: intracranial volume (ICV), and volumes of the hippocampus,
132 entorhinal cortex, and lateral ventricles as well as the latter four divided by the ICV. These features
133 were selected based on previous studies [25]. We included volumes divided by the ICV as it is
134 unclear whether raw or ICV-corrected volumes are better predictors of dementia [25,26]. MR
135 imaging protocol details are provided by ADNI at [http://adni.loni.usc.edu/methods/mri-tool/mri-
136 analysis/](http://adni.loni.usc.edu/methods/mri-tool/mri-analysis/). Cortical reconstruction and volumetric segmentation had been performed with the
137 FreeSurfer 5.1 image analysis suite. A brief description of the processing is provided in the
138 supplementary material (Section B) [27].

139

140 **2.1.3 AV-45 PET**

141 As AV-45 PET features, we used standardized uptake values (SUVs) in four regions: frontal cortex,
142 cingulate, lateral parietal cortex, and lateral temporal cortex. The AV-45 PET measures amyloid-
143 beta load in the brain. AV-45 PET imaging and preprocessing details are available at
144 <http://adni.loni.usc.edu/methods/pet-analysis-method/pet-analysis/> [28]. We used regional SUV
145 ratios processed according to the UC Berkeley protocol [28–30]. Each AV-45 PET scan was co-
146 registered to the corresponding MRI and the mean AV-45 uptake within the regions of interest and
147 reference regions was calculated. Regions of interest were composites of frontal regions,
148 anterior/posterior cingulate regions, lateral parietal regions, and lateral temporal regions [31]. The

149 final PET measurements were the average amyloid-beta uptakes in the four ROIs normalized by the
150 whole cerebellum reference region.

151

152 **2.1.4 FDG PET**

153 As FDG-PET features, we used average SUVs in five brain regions: bilateral angular gyri, bilateral
154 posterior cingulate gyri, and bilateral inferior temporal gyri. The FDG PET data measures glucose
155 consumption and is shown to be strongly related to dementia and cognitive impairment when
156 compared to normal control subjects [30,32,33]. Motion correction and co-registration with MRI
157 was performed on the acquired PET data. The highest 50% of voxel values within a hand-drawn
158 pons/cerebellar vermis region were selected and their mean was used to normalize each ROI
159 measurement resulting in the final FDG PET measurements. Regions of interests were bilateral
160 angular gyri, bilateral posterior cingulate gyri, and bilateral inferior temporal gyri.

161

162 **2.1.5 CSF proteins**

163 The baseline CSF $A\beta_{42}$, t-tau, and p-tau were used as CSF features [34]. CSF was collected in the
164 morning after an overnight fast using a 20- or 24-gauge spinal needle, frozen within 1 hour of
165 collection, and transported on dry ice to the ADNI Biomarker Core laboratory at the University of
166 Pennsylvania Medical Center. The levels of $A\beta_{42}$, t-tau, and p-tau in CSF were used.

167

168 **2.1.6 Neuropsychology and behavioral (NePB) assessments**

169 The NePB assessments reflect the cognitive abilities of the subjects. Subjects underwent a battery of
170 NePB tests [35]. We selected to include 5 NePB scores as NePB features: the summary score from
171 Mini-Mental State Examination (MMSE) [36], three summary scores of Rey's auditory verbal
172 learning test (RAVLT; learning, immediate, and percent forgetting) [37], and a summary score from
173 the functional activities Questionnaire (FAQ) [38].

174

175 **2.1.7 Risk factors: age, education, and APOE**

176 Past studies have found several risk factors contributing to AD [8]. We considered age, the number
177 of APOE e4 alleles, and the years of education. With aging, normal cognitive decline is an accepted
178 phenomenon, but lower education and lower cerebral metabolic activity could accelerate the normal
179 decline [39]. The APOE e4 allele, present in approximately 10-15% of people, increases the risk for
180 late-onset AD and lowers the age of onset. One copy of e4 (e3/e4) can increase risk by 2-3 times
181 while homozygotes (e4/e4) can be at 12 times increased risk [40]. We coded APOE e4 status of
182 absence, single copy or homozygous coded as 0, 1 and 2 respectively.

183

184 **2.1.8 ADAS-cog scores**

185 The ADAS-cog 11 task scale was developed to assess the efficacy of anti-dementia treatments.
186 Further developments to the scale shifted its sensitivity towards pre-dementia syndromes as well,
187 primarily mild cognitive impairment (MCI). The ADAS-cog 13 task scale was one such
188 improvement on the original ADAS-cog 11, with additional memory and attention/executive
189 function tasks [41]. The final 13 tasks test verbal memory (3 tasks), clinician-rated perception (4
190 tasks), and general cognition (6 tasks). It was found to perform better than the ADAS-cog 11 at
191 discriminating between MCI and mild AD patients, as well as have better sensitivity to treatment
192 effects in MCI [42]. As the ADAS-cog 13 fully encompasses the ADAS-cog 11 tasks, it is also
193 backward compatible. As such, we used the ADAS-cog 13 scale for our study as a continuous
194 quantitative measure of a subject's disease status. The scores at baseline, 12-month, 24-month and
195 36-month timelines were obtained from the ADNI dataset (Table S.2). The value (0 to 85) of these
196 scores is lowest for the normal control group and increases with disease progression and the scores
197 are highest for AD subjects.

198

199 2.2 Multivariate regression analysis

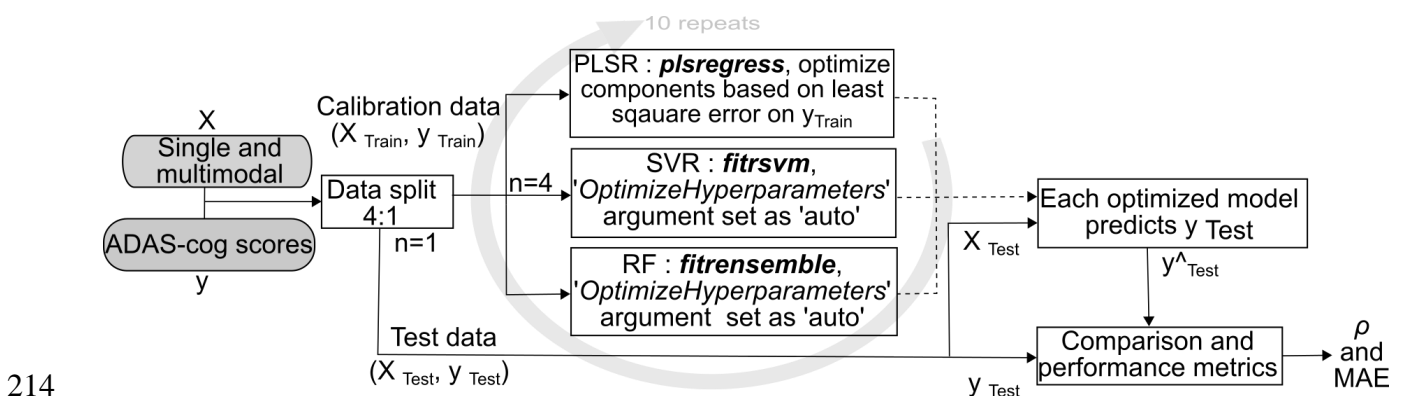
200 We employed multivariate regression to predict ADAS-cog scores based on predictor variables
201 detailed in section 2.1. We considered four different prediction tasks: predicting ADAS-cog score at
202 baseline and at 12, 24, or 36 months after the baseline. In all of these tasks, the predictor variables
203 are from the baseline visit. The group of features (predictors) used for regression are denoted by the
204 column vectors X_i , ($i = 0, 1, \dots, L$), where L is the number of features (Figure S.2). The ADAS-
205 cog scores (dependent variable or response variable) are denoted by the column vector Y .

206

207 We employed widely used machine learning techniques including partial least squares regression
208 (PLSR) [43], support vector regression (SVR) [44], and random forest regression (RF) and created
209 prediction models [45]. Additionally, a genetic algorithm (GA) was utilized to rank the variables in
210 the order of importance in the multi-modal case [46]. The details on these methods are provided in
211 the supplementary section.

212

213 2.3 Regression modeling and performance metrics



214

215 **Figure 1:** Schematic of regression modeling. X is single or multi-modal predictors and Y is the
216 target value to be predicted. We utilized 5-fold cross-validation repeated 10 times to account for the
217 random assignment of subjects to different folds. Partial least squares regression (PLSR), support-
218 vector regression (SVR) and random forest regression (RF) models were trained and tuned based on
219 training folds and evaluated on test folds. The utilized Matlab function and hyperparameter tuning

220 are shown in italics. Cross-validated correlation (ρ) and mean absolute error (MAE) metrics were
221 employed and average performance for 10 runs computed.

222

223 The prediction of the ADAS scores (at baseline, 12-months, 24-months, and 36 months) was
224 performed by employing PLSR, SVR, and RF. Both single modal (each modality of Section 2.1
225 alone) and multi-modal predictors (all modalities of Section 2.1 combined,) were considered. All
226 the predictors were from the baseline visit. We evaluated the prediction models using 5-fold
227 repeated cross-validation with 10 repeats, see **Figure 1** and Figure S.2. Under single modalities
228 Age, years of education (Edu), number of APOE e4 alleles (APOE) were exactly 1 variable each,
229 CSF had 3 variables, AVF45-PET had 4 variables, NePB and FDG had 5 variables each, MRI had 9
230 variables and hence the multimodal model had a total of 29 variables (Figure S.2). All variables
231 were assumed to be continuous and we standardized the variables to be zero-mean and unit standard
232 deviation. The model was evaluated in terms of correlation coefficient (ρ) and the mean absolute
233 error (MAE) between the actual ADAS-cog 13 scores and its model-predicted values. From the 5-
234 fold cross-validation, we averaged the resulting 5 distinct values and computed 95% confidence
235 intervals (CIs) using the bootstrapping method. Similarly, MAE and its CIs were computed. The
236 process was repeated 10 times and its distribution analyzed. For mathematical details of these
237 performance metrics as well as the CI computation in the case of repeated cross-validation that
238 takes into account inter-dependency of distinct repeats, readers may consult Lewis et.al. [47].

239

240 The analyses were performed on MATLAB 2018b (The Mathworks Inc, Natick, MA) using native
241 machine learning functions. The PLSR was executed with *plsregress* function and the optimal
242 number of PLS components was manually selected based on the least root mean square error for
243 training data [48]. SVR was executed with *fitrsvm* and RF with *fitrensemble* and in both methods
244 the models were tuned by setting *OptimizeHyperparameters* argument as *auto* [49,50].

245 Additionally, Additionally, GA-PLS was utilized to analyze the importance of each modality in the
246 multimodal PLSR regression models [51].

247 (The main codes and resulting *.mat* file are available on GitHub:
248 https://github.com/mithp/ADAS_multimodal.git)

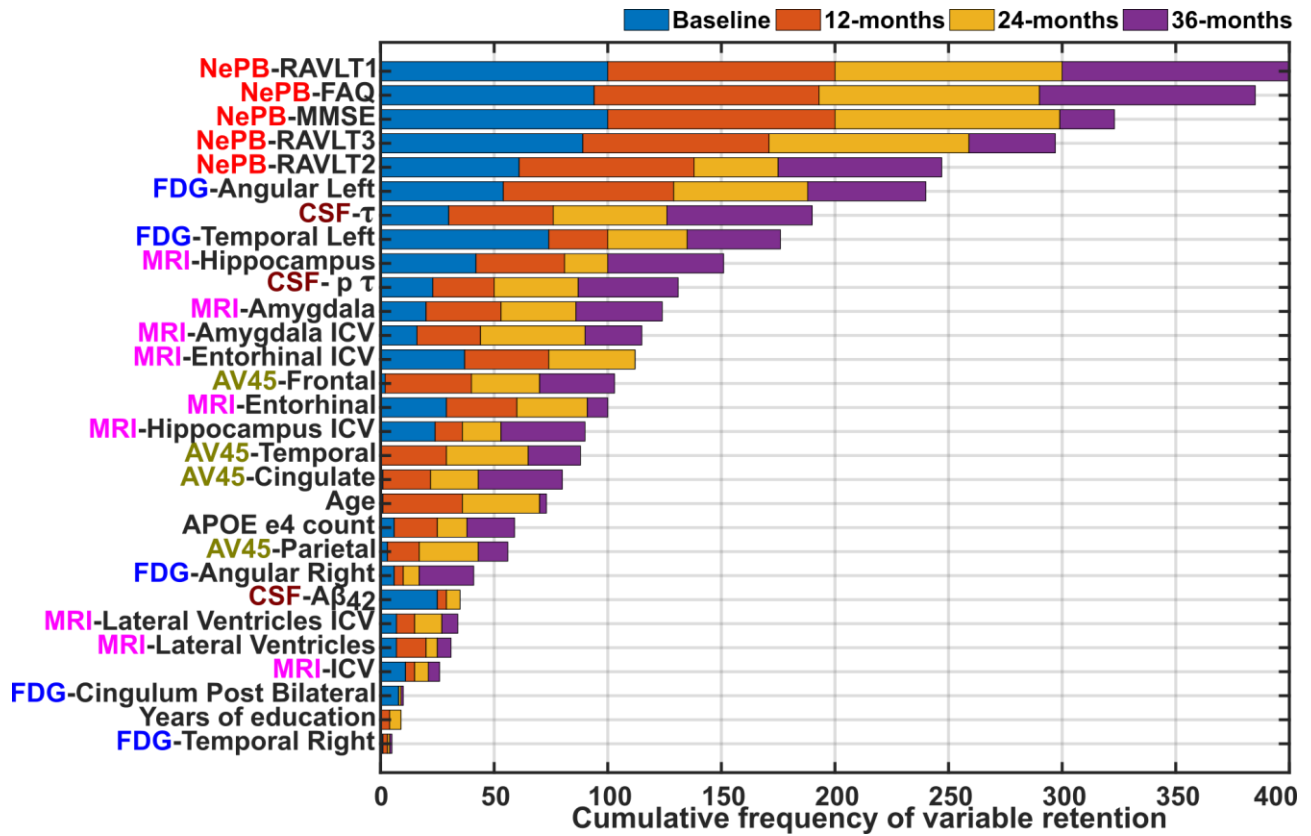
249

250 **3 Results**

251 As depicted in **Figure 1**, we created single modality and multi-modal regression models and
252 compared their performance. The comparison (**Figure 3**) shows that multi-modal based prediction
253 models outperform single modality consistently in all the timelines (baseline and subsequent 12, 24
254 and 36-month follow-up) in all subjects tested (i.e., collapsing over diagnostic categories). The
255 correlation between the predicted ADAS-Cog 13 based on multi-modal data and that observed at
256 12, 24 and 36 months, reached 0.86, 0.82, and 0.75, respectively. The performance comparison
257 (Figure S.3) shows that the differences among PLSR, SVR, and RF were not significant (i.e., $p >$
258 0.05), except for some instances where PLSR underperformed compared to RF (baseline and 12
259 months: MRI, CSF, and FDG; 24 and 36 months: APOE and multi-modal). However, PLSR models
260 were computationally faster and performed consistently.

261

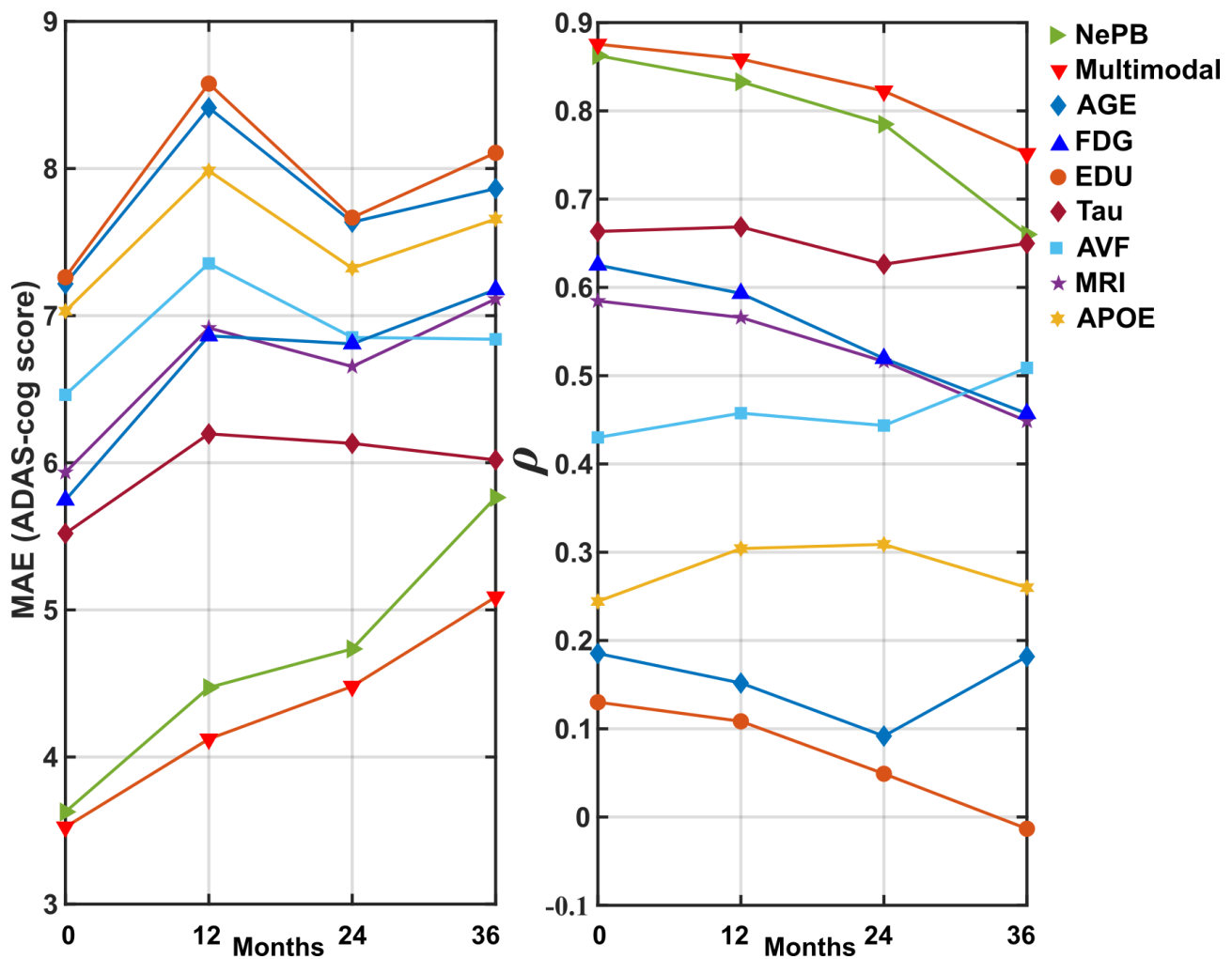
262 By analyzing the importance of measures (**Figure 2**) contributing to PLSR's correlation we observe
263 that the neuropsychological and behavioral parameters (NePB) were most important and consistent
264 across time periods for predicting ADAS score, followed by CSF and MRI biomarkers. Despite the
265 association of age at baseline, years of education (Edu.) and APOE e4 status with AD risk, these
266 parameters were found to be least important, perhaps because these factors are somehow reflected
267 in other parameters. By contrast, the importance of amyloid and τ increased when predictions were
268 made 36 months in advance (**Figure 2**). Additionally, metabolic activity in temporal right and left
269 sides were on the opposite ends of the importance in the ADAS-cog score predictions.



270

271 **Figure 2:** Genetic algorithm-based importance of parameters in correlations as observed for 100
 272 runs for every time period. The frequency indicates the proportional contribution in ADAS-cog 13
 273 score prediction. The modality group is prefixed to the variable names.

274



275

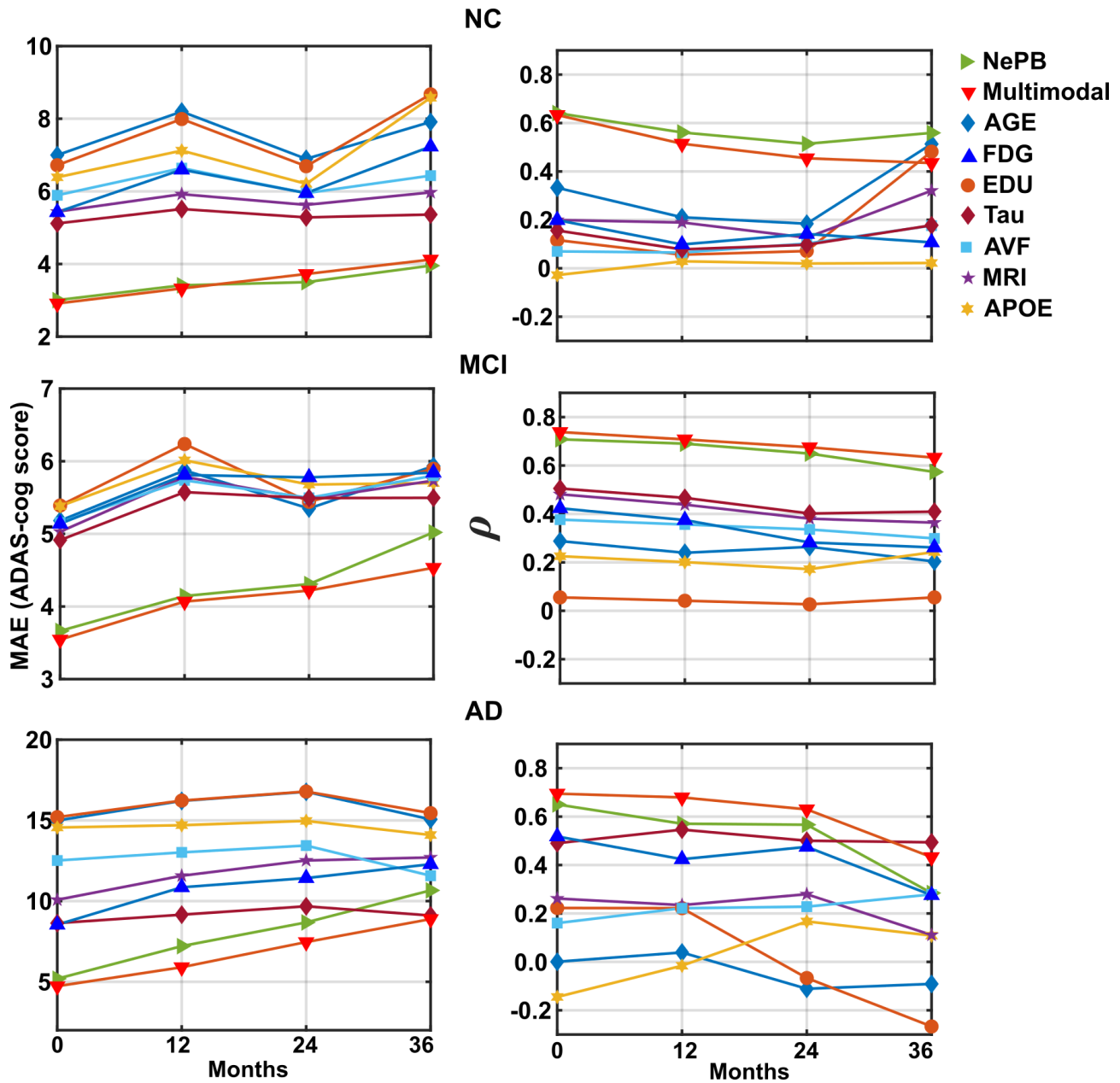
276 **Figure 3:** Comparison of single and multi-modal dataset performance – collapsing across
 277 diagnostic status – with partial least squares regression. The performance measures cross-validation
 278 correlation (ρ) and mean absolute error (MAE) for ADAS-cog scores are plotted for predictions at
 279 0, 12, 24 and 36 months in advance.

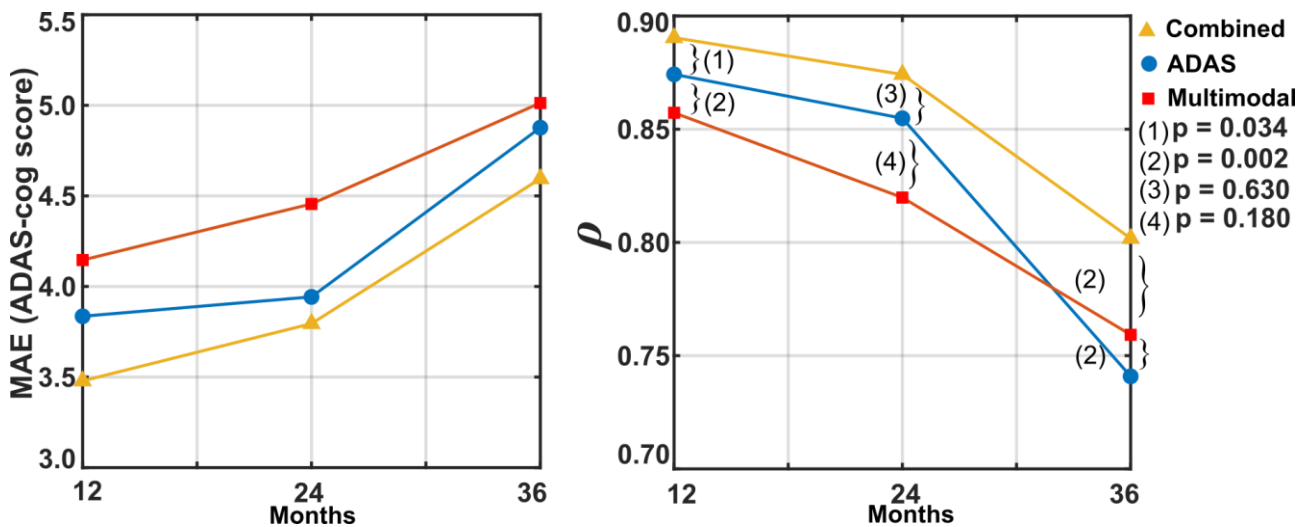
280

281 Grouping data based on diagnosis at baseline (**Figure 4**) and analyzing the performance further
 282 magnified the poor correlation when a single modality approach was employed to predict this multi-
 283 factorial disease. We observe that NePB, single modal, data shows the best predictive performance,
 284 in keeping with the fact that the to-be-predicted variable (ADAS-Cog 13) also contains NeBP
 285 outcomes. However, the multimodal approach performs better than MCI and AD groups especially

286 during 24- and 36-month time periods. Due to the high variation in ADAS scores in AD groups the
287 correlation (ρ) and MAE were not inversely proportional to each other.

288

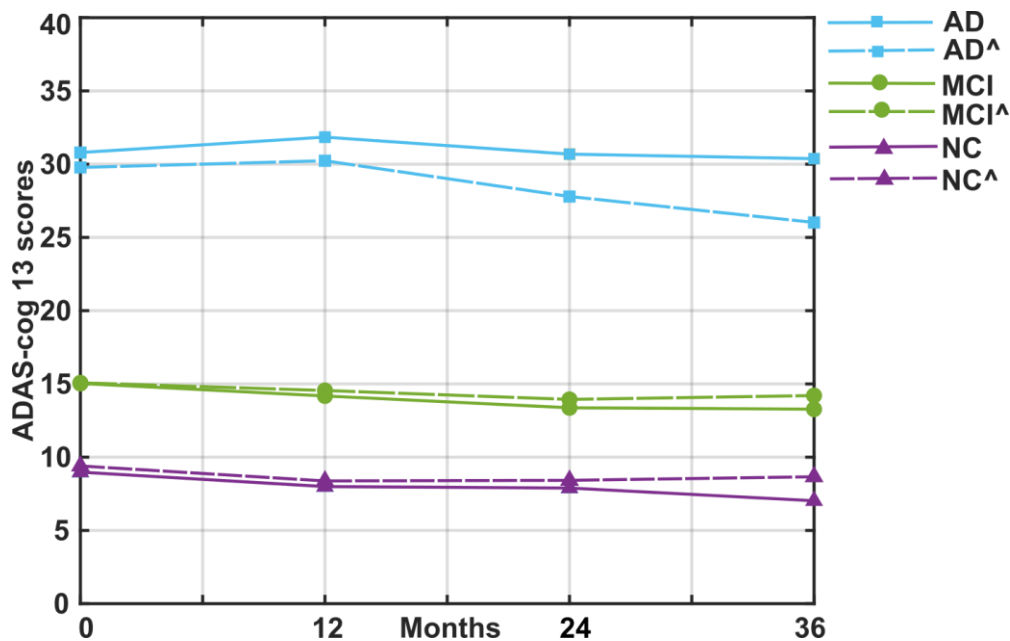




294

295 **Figure 5:** Performance comparison of prediction models utilizing only ADAS scores vs.
 296 multimodal data with and without the combination with baseline ADAS scores. The p-values
 297 correspond to pair-wise differences between the three prediction models at different time periods.

298



299

300 **Figure 6:** The mean of actual ADAS-cog 13 scores of subjects over 36 months is plotted (solid line)
 301 for the 3 diagnostic groups (normal cognition (NC), mild cognitive impairment (MCI) and
 302 Alzheimer's disease (AD)). The learning model predicted scores for these time periods are also
 303 plotted (dashed lines) for each diagnostic group (model predictions indicated with a caret (^)
 304 symbol).

305

306 Our multimodal approach (multivariate) based prediction models with the inclusion of baseline
307 ADAS-cog scores were better ($\rho = 0.80$ to 0.90 , **Figure 5**) than prediction models based only on
308 baseline ADAS-cog scores (univariate, $\rho = 0.75$ to 0.87). The inclusion of the ADAS-cog score
309 with other baseline multi-modal predictors was observed with improvements ($p = 0.002$ to 0.18) in
310 the correlations. Overall, the prediction models predict well across the time periods and this can be
311 observed when we compare the mean predicted values versus the actual mean values (**Figure 6**).

312

313 **4 Discussion**

314 We present a multi-modal regression approach to quantitatively track the progression of
315 Alzheimer's disease and show that it outperforms the conventional single modal approach.
316 Quantification of AD aids clinicians in decisions with treatment and a multi-modal approach
317 ensures that the prediction models consider all biomarkers contributing to the disease condition.
318 Furthermore, conventional classification of patients into normal, MCI or AD could be avoided as a
319 clear distinction amongst the group is a challenging task [52].

320

321 The classification of subjects based on a few modalities has been the focus of most recent studies.
322 Although high classification accuracy ($>80\%$) has been reported [11], we speculate that the impact
323 of mislabeling a subject in the wrong category (and hence, wrong therapy prescribed) is higher than
324 the error in predicting ADAS-cog scores (<5 units). Additionally, ADAS-cog scores are easy to
325 interpret and follow the longitudinal tracking of AD progression. In agreement with the
326 classification-based studies [4], the multi-modal approach outperforms the single modality,
327 however, in this study multi-modal data were used for predicting the ADAS-cog scores.
328 Furthermore, our multi-modal approach shows that ADAS-cog scores are conducive to longitudinal
329 predictions contrary to Marinescu et al [21], where ADAS-cog scores were concluded not

330 predictable. We, however, acknowledge that studies were not set up equally as there were time
331 constraints, differences in subjects and underutilization of longitudinal data.

332

333 Clinically, NePB tests and ADAS-cog scores measure the subject's cognitive abilities and this
334 similarity was showcased with the observance of higher correlations (**Figure 3**). CSF biomarkers
335 showed high correlations several studies support this strong relationship between CSF biomarkers
336 and AD state [34]. As the precise pathophysiology and relative contribution of different pathogenic
337 factors to AD at different phases of disease progression are currently still under investigation, the
338 results advocate that instead of manually estimating the best markers, a multi-modal approach is
339 beneficial. However, we acknowledge that the variable selection methods can be utilized to select
340 the best AD measures (or create sparse models) utilized in multimodal modeling further improving
341 the robustness of the prediction model.

342

343 The multivariate techniques (i.e., PLSR, SVR, and RF) were observed to perform very similarly in
344 their predictions but the computation times were different, and this prompted us to favor PLSR.
345 Other nonlinear model selection techniques could improve current results [53]. The subject attrition
346 during follow-ups may have diminished the predictive performance of the model.

347

348 **5 Conclusion**

349 ADAS-cog 13 scores reflect the current cognitive state of individuals, and through multivariate
350 regression and a multi-modal dataset, our results show that quantitative longitudinal prediction of
351 AD progression is possible. Thus, the automated multi-modal approach may help clinicians make
352 timely decisions for interventions at all stages of AD and inform likely disease progression at the
353 start of clinical trials.

354

355 **6 References**

- 356 [1] Gaudreault R, Mousseau N. Mitigating Alzheimer's Disease with Natural Polyphenols: A
357 Review. *Curr Alzheimer Res* 2019;16:529–43.
358 <https://doi.org/10.2174/1567205016666190315093520>.
- 359 [2] Association A. 2019 Alzheimer's disease facts and figures. *Alzheimer's Dement*
360 2019;15:321–87. <https://doi.org/10.1016/j.jalz.2019.01.010>.
- 361 [3] Mueller SG, Weiner MW, Thal LJ, Petersen RC, Jack CR, Jagust W, et al. Ways toward an
362 early diagnosis in Alzheimer's disease: The Alzheimer's Disease Neuroimaging Initiative
363 (ADNI). *Alzheimer's Dement* 2005;1:55–66. <https://doi.org/10.1016/j.jalz.2005.06.003>.
- 364 [4] Zhang D, Wang Y, Zhou L, Yuan H, Shen D. Multimodal classification of Alzheimer's
365 disease and mild cognitive impairment. *Neuroimage* 2011;55:856–67.
366 <https://doi.org/10.1016/j.neuroimage.2011.01.008>.
- 367 [5] Perry RJ, Watson P, Hodges JR. The nature and staging of attention dysfunction in early
368 (minimal and mild) Alzheimer's disease: Relationship to episodic and semantic memory
369 impairment. *Neuropsychologia* 2000;38:252–71. [https://doi.org/10.1016/S0028-](https://doi.org/10.1016/S0028-3932(99)00079-2)
370 [3932\(99\)00079-2](https://doi.org/10.1016/S0028-3932(99)00079-2).
- 371 [6] Morris JC, Storandt M, Miller JP, McKeel DW, Price JL, Rubin EH, et al. Mild cognitive
372 impairment represents early-stage Alzheimer disease. *Arch Neurol* 2001;58:397–405.
373 <https://doi.org/10.1001/archneur.58.3.397>.
- 374 [7] Nestor PJ, Scheltens P, Hodges JR. Advances in the early detection of alzheimer's disease.
375 *Nat Rev Neurosci* 2004;10:S34. <https://doi.org/10.1038/nrn1433>.
- 376 [8] Duara R, Barker WW, Lopez-Alberola R, Loewenstein DA, Grau LB, Gilchrist D, et al.
377 Alzheimer's disease: Interaction of apolipoprotein E genotype, family history of dementia,
378 gender, education, ethnicity, and age of onset. *Neurology* 1996;46:1575–9.
379 <https://doi.org/10.1212/WNL.46.6.1575>.

- 380 [9] Selkoe DJ. The molecular pathology of Alzheimer's disease. *Neuron* 1991;6:487–98.
381 [https://doi.org/10.1016/0896-6273\(91\)90052-2](https://doi.org/10.1016/0896-6273(91)90052-2).
- 382 [10] Teipel S, Drzezga A, Grothe MJ, Barthel H, Chételat G, Schuff N, et al. Multimodal imaging
383 in Alzheimer's disease: Validity and usefulness for early detection. *Lancet Neurol*
384 2015;14:1037–53. [https://doi.org/10.1016/S1474-4422\(15\)00093-9](https://doi.org/10.1016/S1474-4422(15)00093-9).
- 385 [11] Rathore S, Habes M, Iftikhar MA, Shacklett A, Davatzikos C. A review on neuroimaging-
386 based classification studies and associated feature extraction methods for Alzheimer's
387 disease and its prodromal stages. *Neuroimage* 2017;155:530–48.
388 <https://doi.org/10.1016/j.neuroimage.2017.03.057>.
- 389 [12] Jack CR, Knopman DS, Jagust WJ, Petersen RC, Weiner MW, Aisen PS, et al. Tracking
390 pathophysiological processes in Alzheimer's disease: An updated hypothetical model of
391 dynamic biomarkers. *Lancet Neurol* 2013;12:207–16. [https://doi.org/10.1016/S1474-4422\(12\)70291-0](https://doi.org/10.1016/S1474-4422(12)70291-0).
- 393 [13] Keihaninejad S, Zhang H, Ryan NS, Malone IB, Modat M, Cardoso MJ, et al. An unbiased
394 longitudinal analysis framework for tracking white matter changes using diffusion tensor
395 imaging with application to Alzheimer's disease. *Neuroimage* 2013;72:153–63.
396 <https://doi.org/10.1016/j.neuroimage.2013.01.044>.
- 397 [14] Jack CR, Holtzman DM. Biomarker modeling of alzheimer's disease. *Neuron* 2013;80:1347–
398 58. <https://doi.org/10.1016/j.neuron.2013.12.003>.
- 399 [15] Growdon JH. Incorporating biomarkers into clinical drug trials in Alzheimer's disease. *J*
400 *Alzheimers Dis* 2001;3:287–92. <https://doi.org/10.3233/jad-2001-3303>.
- 401 [16] Yang E, Farnum M, Lobanov V, Schultz T, Raghavan N, Samtani MN, et al. Quantifying the
402 pathophysiological timeline of Alzheimer's disease. *J Alzheimer's Dis* 2011;26:745–53.
403 <https://doi.org/10.3233/JAD-2011-110551>.
- 404 [17] William-Faltaos D, Chen Y, Wang Y, Gobburu J, Zhu H. Quantification of disease

- 405 progression and dropout for Alzheimer’s disease. *Int J Clin Pharmacol Ther* 2013;51:120–31.
406 <https://doi.org/10.5414/CP201787>.
- 407 [18] Skinner J, Carvalho JO, Potter GG, Thames A, Zelinski E, Crane PK, et al. The Alzheimer’s
408 Disease Assessment Scale-Cognitive-Plus (ADAS-Cog-Plus): An expansion of the ADAS-
409 Cog to improve responsiveness in MCI. *Brain Imaging Behav* 2012;6:489–501.
410 <https://doi.org/10.1007/s11682-012-9166-3>.
- 411 [19] Kueper JK, Speechley M, Montero-Odasso M. The Alzheimer’s Disease Assessment Scale-
412 Cognitive Subscale (ADAS-Cog): Modifications and Responsiveness in Pre-Dementia
413 Populations. A Narrative Review. *J Alzheimer’s Dis* 2018;63:423–44.
414 <https://doi.org/10.3233/JAD-170991>.
- 415 [20] Zhang D, Shen D. Predicting Future Clinical Changes of MCI Patients Using Longitudinal
416 and Multimodal Biomarkers. *PLoS One* 2012;7:e33182.
417 <https://doi.org/10.1371/journal.pone.0033182>.
- 418 [21] Marinescu R V., Oxtoby NP, Young AL, Bron EE, Toga AW, Weiner MW, et al. TADPOLE
419 Challenge: Accurate Alzheimer’s Disease Prediction Through Crowdsourced Forecasting of
420 Future Data, 2019, p. 1–10. https://doi.org/10.1007/978-3-030-32281-6_1.
- 421 [22] Steenland K, Zhao L, Goldstein F, Cellar J, Lah J. Biomarkers for predicting cognitive
422 decline in those with normal cognition. *J Alzheimers Dis* 2014;40:587–94.
423 <https://doi.org/10.3233/JAD-2014-131343>.
- 424 [23] Bengtson JF, Balsis S, Geraci L, Massman PJ, Doody RS. How well do the ADAS-cog and its
425 subscales measure cognitive dysfunction in Alzheimer’s disease? *Dement Geriatr Cogn*
426 *Disord* 2009;28:63–9. <https://doi.org/10.1159/000230709>.
- 427 [24] Marinescu R V., Oxtoby NP, Young AL, Bron EE, Toga AW, Weiner MW, et al. TADPOLE
428 Challenge: Prediction of Longitudinal Evolution in Alzheimer’s Disease 2018.
- 429 [25] Gómez-Sancho M, Tohka J, Gómez-Verdejo V. Comparison of feature representations in

- 430 MRI-based MCI-to-AD conversion prediction. *Magn Reson Imaging* 2018;50:84–95.
431 <https://doi.org/10.1016/j.mri.2018.03.003>.
- 432 [26] Voevodskaya O. The effects of intracranial volume adjustment approaches on multiple
433 regional MRI volumes in healthy aging and Alzheimer’s disease. *Front Aging Neurosci*
434 2014;6. <https://doi.org/10.3389/fnagi.2014.00264>.
- 435 [27] Reuter M, Schmansky NJ, Rosas HD, Fischl B. Within-subject template estimation for
436 unbiased longitudinal image analysis. *Neuroimage* 2012;61:1402–18.
437 <https://doi.org/10.1016/j.neuroimage.2012.02.084>.
- 438 [28] Johnson KA, Sperling RA, Gidicsin CM, Carmasin JS, Maye JE, Coleman RE, et al.
439 Florbetapir (F18-AV-45) PET to assess amyloid burden in Alzheimer’s disease dementia,
440 mild cognitive impairment, and normal aging. *Alzheimer’s Dement* 2013;9.
441 <https://doi.org/10.1016/j.jalz.2012.10.007>.
- 442 [29] Landau SM, Mintun MA, Joshi AD, Koeppe RA, Petersen RC, Aisen PS, et al. Amyloid
443 deposition, hypometabolism, and longitudinal cognitive decline. *Ann Neurol* 2012;72:578–
444 86. <https://doi.org/10.1002/ana.23650>.
- 445 [30] Landau SM, Lu M, Joshi AD, Pontecorvo M, Mintun MA, Trojanowski JQ, et al. Comparing
446 positron emission tomography imaging and cerebrospinal fluid measurements of β -amyloid.
447 *Ann Neurol* 2013;74:826–36. <https://doi.org/10.1002/ana.23908>.
- 448 [31] Mormino EC, Kluth JT, Madison CM, Rabinovici GD, Baker SL, Miller BL, et al. Episodic
449 memory loss is related to hippocampal-mediated β -amyloid deposition in elderly subjects.
450 *Brain* 2009;132:1310–23. <https://doi.org/10.1093/brain/awn320>.
- 451 [32] Landau SM, Harvey D, Madison CM, Koeppe RA, Reiman EM, Foster NL, et al.
452 Associations between cognitive, functional, and FDG-PET measures of decline in AD and
453 MCI. *Neurobiol Aging* 2011;32:1207–18.
454 <https://doi.org/10.1016/j.neurobiolaging.2009.07.002>.

- 455 [33] Jagust WJ, Bandy D, Chen K, Foster NL, Landau SM, Mathis CA, et al. The Alzheimer's
456 Disease Neuroimaging Initiative positron emission tomography core. *Alzheimer's Dement*
457 2010;6:221–9. <https://doi.org/10.1016/j.jalz.2010.03.003>.
- 458 [34] Shaw LM, Vanderstichele H, Knapik-Czajka M, Clark CM, Aisen PS, Petersen RC, et al.
459 Cerebrospinal fluid biomarker signature in alzheimer's disease neuroimaging initiative
460 subjects. *Ann Neurol* 2009;65:403–13. <https://doi.org/10.1002/ana.21610>.
- 461 [35] Battista P, Salvatore C, Castiglioni I. Optimizing neuropsychological assessments for
462 cognitive, behavioral, and functional impairment classification: A machine learning study.
463 *Behav Neurol* 2017;2017. <https://doi.org/10.1155/2017/1850909>.
- 464 [36] Folstein MF, Folstein SE, McHugh PR. "Mini-mental state". A practical method for grading
465 the cognitive state of patients for the clinician. *J Psychiatr Res* 1975;12:189–98.
466 [https://doi.org/10.1016/0022-3956\(75\)90026-6](https://doi.org/10.1016/0022-3956(75)90026-6).
- 467 [37] Rey A. *L'examen clinique en psychologie*. Press Univ Fr 1958.
468 <https://psycnet.apa.org/record/1959-03776-000> (accessed December 30, 2019).
- 469 [38] Pfeffer RI, Kurosaki TT, Harrah CH, Chance JM, Filos S. Measurement of functional
470 activities in older adults in the community. *Journals Gerontol* 1982;37:323–9.
471 <https://doi.org/10.1093/geronj/37.3.323>.
- 472 [39] Prencipe M, Casini AR, Ferretti C, Lattanzio MT, Fiorelli M, Culasso F. Prevalence of
473 dementia in an elderly rural population: effects of age, sex, and education. *J Neurol*
474 *Neurosurg Psychiatry* 1996;60:628–33. <https://doi.org/10.1136/jnnp.60.6.628>.
- 475 [40] Michaelson DM. APOE ε4: The most prevalent yet understudied risk factor for Alzheimer's
476 disease. *Alzheimer's Dement* 2014;10:861–8. <https://doi.org/10.1016/j.jalz.2014.06.015>.
- 477 [41] Mohs RC, Knopman D, Petersen RC, Ferris SH, Ernesto C, Grundman M, et al.
478 Development of cognitive instruments for use in clinical trials of antidementia drugs:
479 Additions to the Alzheimer's disease assessment scale that broaden its scope. *Alzheimer Dis*

- 480 Assoc Disord 1997;11. <https://doi.org/10.1097/00002093-199700112-00003>.
- 481 [42] Raghavan N, Samtani MN, Farnum M, Yang E, Novak G, Grundman M, et al. The ADAS-
482 Cog revisited: Novel composite scales based on ADAS-Cog to improve efficiency in MCI
483 and early AD trials. *Alzheimer's Dement* 2013;9. <https://doi.org/10.1016/j.jalz.2012.05.2187>.
- 484 [43] Krishnan A, Williams LJ, McIntosh AR, Abdi H. Partial Least Squares (PLS) methods for
485 neuroimaging: A tutorial and review. *Neuroimage* 2011;56:455–75.
486 <https://doi.org/10.1016/j.neuroimage.2010.07.034>.
- 487 [44] Zhang D, Shen D. Multi-modal multi-task learning for joint prediction of multiple regression
488 and classification variables in Alzheimer's disease. *Neuroimage* 2012;59:895–907.
489 <https://doi.org/10.1016/j.neuroimage.2011.09.069>.
- 490 [45] Gray KR, Aljabar P, Heckemann RA, Hammers A, Rueckert D. Random forest-based
491 similarity measures for multi-modal classification of Alzheimer's disease. *Neuroimage*
492 2013;65:167–75. <https://doi.org/10.1016/j.neuroimage.2012.09.065>.
- 493 [46] Leardi R, Boggia R, Terrile M. Genetic algorithms as a strategy for feature selection. *J*
494 *Chemom* 1992;6:267–81. <https://doi.org/10.1002/cem.1180060506>.
- 495 [47] Lewis JD, Evans AC, Tohka J. T1 white/gray contrast as a predictor of chronological age,
496 and an index of cognitive performance. *Neuroimage* 2018;173:341–50.
497 <https://doi.org/10.1016/j.neuroimage.2018.02.050>.
- 498 [48] de Jong S. SIMPLS: An alternative approach to partial least squares regression. *Chemom*
499 *Intell Lab Syst* 1993;18:251–63. [https://doi.org/10.1016/0169-7439\(93\)85002-X](https://doi.org/10.1016/0169-7439(93)85002-X).
- 500 [49] Breiman L. Bagging predictors. *Mach Learn* 1996;24:123–40.
501 <https://doi.org/10.1007/BF00058655>.
- 502 [50] Breiman L. Random forests. *Mach Learn* 2001;45:5–32.
503 <https://doi.org/10.1023/A:1010933404324>.
- 504 [51] R. Leardi and A. Lupiáñez. Genetic algorithms applied to feature selection in PLS regression:

505 how and when to use them. *Chemom Intell Lab Syst* 1998;41:95–207.

506 [52] Leyhe T, Reynolds CF, Melcher T, Linnemann C, Klöppel S, Blennow K, et al. A common
507 challenge in older adults: Classification, overlap, and therapy of depression and dementia.

508 *Alzheimer's Dement* 2017;13:59–71. <https://doi.org/10.1016/j.jalz.2016.08.007>.

509 [53] Chouldechova A, Hastie T. Generalized Additive Model Selection. *ArXiv Prepr*
510 *ArXiv150603850* 2015.

511

512 **7 Figure legends**

513 **Figure 1:** Schematic of regression modeling. X is single or multi-modal predictors and Y is the
514 target value to be predicted. We utilized 5-fold cross-validation repeated 10 times to account for the
515 random assignment of subjects to different folds. Partial least squares regression (PLSR), support-
516 vector regression (SVR) and random forest regression (RF) models were trained and tuned based on
517 training folds and evaluated on test folds. The utilized Matlab function and hyperparameter tuning
518 are shown in italics. Cross-validated correlation (ρ) and mean absolute error (MAE) metrics were
519 employed and average performance for 10 runs computed.

520

521 **Figure 2:** Genetic algorithm-based importance of parameters in correlations as observed for 100
522 runs for every time period. The frequency indicates the proportional contribution in ADAS-cog 13
523 score prediction. The modality group is prefixed to the variable names.

524

525 **Figure 3:** Comparison of single and multi-modal dataset performance – collapsing across
526 diagnostic status – with partial least squares regression. The performance measures cross-validation
527 correlation (ρ) and mean absolute error (MAE) for ADAS-cog scores are plotted for predictions at
528 0, 12, 24 and 36 months in advance.

529

530 **Figure 4:** Performance of PLSR on single- and multi-modal data stratified according to baseline
531 clinical diagnosis [normal cognition (NC), mild cognitive impairment (MCI) and Alzheimer's
532 disease (AD)]. The performance measures cross-validation correlation (ρ) and mean absolute error
533 (MAE) for ADAS-cog scores are plotted for predictions at 0, 12, 24 and 36 months in advance.

534

535 **Figure 5:** Performance comparison of prediction models utilizing only ADAS scores vs.
536 multimodal data with and without the combination with baseline ADAS scores. The p-values
537 correspond to pair-wise differences between the three prediction models at different time periods.

538

539 **Figure 6:** The mean of actual ADAS-cog 13 scores of subjects over 36 months is plotted (solid line)
540 for the 3 diagnostic groups (normal cognition (NC), mild cognitive impairment (MCI) and
541 Alzheimer's disease (AD)). The learning model predicted scores for these time periods are also
542 plotted (dashed lines) for each diagnostic group (model predictions indicated with a caret (^)
543 symbol).

544

545

546 **Figures in supplementary section**

547

548 **Figure S.1:** The mean ADAS-cog 13 scores of subjects for different time periods and conversion of
549 subjects in different categories. The subjects are grouped by the diagnosis as normal cognition
550 (NC), mild cognitive impairment (MCI) and Alzheimer's disease (AD).

551

552 **Figure S.2:** Regression modeling structure. Single modality uses one predictor at a time while
553 multi-modal uses all the predictors as indicated above. The sample size for baseline (N = 757), 12-
554 months (N = 629), 24-months (N = 563) and 36-months (N = 314) were different due to missing

555 values (cohort attrition). The predictors consist of age at baseline, years of formal education (Edu.),
556 APOE e4 status (absence, single copy or homozygous coded as 0, 1 and 2 respectively), MRI-
557 derived parameters, neuropsychiatric and behavioral assessment (NePB), AV45-PET
558 measurements, CSF biomarkers (amyloid- β , τ , p τ) and FDG-PET measures. The number of features
559 is indicated above each modality abbreviations. All the variables were considered as continuous and
560 standardized to be zero-mean and unit standard deviation.

561

562 **Figure S.3:** Comparison of single and multi-modal dataset performance – collapsing across
563 diagnostic status – with partial least squares regression (PLSR), support-vector regression (SVR)
564 and random forest regression (RF). The performances are shown for cross-validation correlation (ρ)
565 and mean absolute error (MAE).

566

567 **Figure S.4:** Genetic algorithm-based importance of parameters in contributing to increasing
568 correlation as observed for 100 runs for the 36-month time period. The frequency indicates the
569 proportional contribution in ADAS-cog 13 score prediction.

570

571 **8 Table legends**

572

573 **Table S.1:** Specific variable names from the TADPOLE D1_D2 dataset (1 to 5, details as in
574 TADPOLE_D1_D2_Dict.csv) and FDG-PET from UCBERKELEYFDG_07_30_15 table.

575

576 **Table S.2:** Summary of the subject demographics and ADAS-cog 13 scores.

577

578 **Acknowledgments**

579 This study was funded by the Research Committee of the Kuopio University Hospital Catchment
580 Area for the State Research Funding (5041778) and The Finnish Foundation for Technology
581 Promotion (8193, 6227) as well as The Academy of Finland (grant 316258 to JT).

582

583 Data collection and sharing for this project was funded by the Alzheimer's Disease Neuroimaging
584 Initiative (ADNI) (National Institutes of Health Grant U01 AG024904) and DOD ADNI
585 (Department of Defense award number W81XWH-12-2-0012). ADNI is funded by the National
586 Institute on Aging, the National Institute of Biomedical Imaging and Bioengineering, and through
587 generous contributions from the following: AbbVie, Alzheimer's Association; Alzheimer's Drug
588 Discovery Foundation; Araclon Biotech; BioClinica, Inc.; Biogen; Bristol-Myers Squibb Company;
589 CereSpir, Inc.; Cogstate; Eisai Inc.; Elan Pharmaceuticals, Inc.; Eli Lilly and Company;
590 EuroImmun; F. Hoffmann-La Roche Ltd and its affiliated company Genentech, Inc.; Fujirebio; GE
591 Healthcare; IXICO Ltd.; Janssen Alzheimer Immunotherapy Research & Development, LLC.;
592 Johnson & Johnson Pharmaceutical Research & Development LLC.; Lumosity; Lundbeck; Merck
593 & Co., Inc.; Meso Scale Diagnostics, LLC.; NeuroRx Research; Neurotrack Technologies; Novartis
594 Pharmaceuticals Corporation; Pfizer Inc.; Piramal Imaging; Servier; Takeda Pharmaceutical
595 Company; and Transition Therapeutics. The Canadian Institutes of Health Research is providing
596 funds to support ADNI clinical sites in Canada. Private sector contributions are facilitated by the
597 Foundation for the National Institutes of Health (www.fnih.org). The grantee organization is the
598 Northern California Institute for Research and Education, and the study is coordinated by the
599 Alzheimer's Therapeutic Research Institute at the University of Southern California. ADNI data are
600 disseminated by the Laboratory for Neuro Imaging at the University of Southern California.

601

602 This work made use of the TADPOLE data sets <https://tadpole.grand-challenge.org> constructed by

603 the EuroPOND consortium <http://europond.eu> funded by the European Union's Horizon 2020
604 research and innovation program under grant agreement No 666992. The computational analysis
605 was run on the servers provided by Bioinformatics Center, University of Eastern Finland, Finland.

606

607 **9 Highlights**

- 608 • A quantitative approach to track Alzheimer's disease.
- 609 • The multi-modal approach enabled predicting ADAS-cog scores from 12 to 36 months.
- 610 • The combination of multimodal data and baseline ADAS scores enhanced the predictions of future
611 timelines.

612

613 **10 Authors contributions**

614 **Prakash, M.:** Algorithm design and Data analysis.

615 **Abdelaziz, M.:** Data analysis.

616 **Zhang, L. and Strange, B.:** Clinical validation and supervision.

617 **Tohka, J.:** Study design and conception.

618 All authors contributed to the preparation and approval of the final submitted manuscript.

619

620 **11 Conflict of Interest**

621 The authors have no conflicts of interest related to the execution of this study and the preparation of
622 the manuscript.

623